PAPER • OPEN ACCESS

Synthesis and characterization of zinc-imidazolate coordination polymer and its use for photocatalytic degradation of methylene blue dye under visible light irradiation

To cite this article: Mostafa Mohsen *et al* 2020 *IOP Conf. Ser.: Mater. Sci. Eng.* **975** 012012

View the article online for updates and enhancements.

245th ECS Meeting
San Francisco, CA
May 26–30, 2024

PRiME 2024
Honolulu, Hawaii
October 6–11, 2024

Bringing together industry, researchers, and government across 50 symposia in electrochemistry and solid state science and technology

Learn more about ECS Meetings at
http://www.electrochem.org/upcoming-meetings

Save the Dates for future ECS Meetings!

Synthesis and characterization of zinc-imidazolate coordination polymer and its use for photocatalytic degradation of methylene blue dye under visible light irradiation

Mostafa Mohsen[1, 2], Ibrahim Naeem[1], Mohamed I. Awaad[1] and Ahmad Baraka[1]

[1] Chemical Engineering Department, Military Technical College, Kobry Elkobbah, Cairo, Egypt
[2] the corresponding author Moustafa.klm@gmail.com

Abstract. Zinc-Imidazole coordination polymer (Zn-Im CP) was facilely synthesized by hydrothermal method from zinc acetate and imidazole as ligand. The structure of the synthesized Zn-Im CP was analyzed by using scanning electron microscopy (SEM), EDX, FTIR, and powder X-ray diffraction (PXRD). Surface area of Zn-Im CP was determined by BET analysis of N_2 adsorption. The photocatalytic performance of Zn-Im CP using visible light irradiation source was investigated using UV–Vis spectrophotometer for the degradation of methylene blue. The pseudo first order reaction kinetic model was applied on the degradation data which gave the rate constant of 0.006 min^{-1}. The results indicate that Zn-Im CP exhibits good photocatalytic performance for the photodegradation of methylene blue following indirect mechanism pathway.
Keywords: Photocatalytic degradation, Visible light, Coordination polymer, Dye, imidazole.

1. Introduction
Textile industry and alike produce dyes effluents with a serious environmental impact due to their toxicity and carcinogenic effect and they show persistency because of difficulty of natural degradation. Various methods have been suggested to handle the dye removal from waters including biodegradation, coagulation, adsorption, advanced oxidation process and membrane–based separation processes. The short comings inherited in the preceding processes drive researchers in the last decade to explore extensively the field of photocatalysis and to continually develop new photocatalysts for the degradation of organic pollutants, especially dyes, in wastewater and effluents[1, 2]. Photocatalysis process is a common and clean method for water decontamination from different pollutants such as organic dyes. It has several advantages over other decontamination methods such as the use of the natural oxidant (O_2), its action at normal conditions (temperature and pressure),ease separation of catalysts and its availability for recycling[3].

Classical semiconductors such as TiO_2, ZnO, and CuO have proved their good photocatalytic properties in the degradation of organic dyes such as methylene blue (MB), methyl orange (MO), rhodamine B (RHB), and other hazardous materials. The band gaps (BG) of TiO_2 and ZnO are 3.2 and 3.17 eV respectively. Therefore, such catalysts are only active under irradiation with ultraviolet light ($\lambda < 387$)[3, 4].The development of new visible light photocatalytic materials, characterized by narrow band gaps, is a pressing demand in the field of photocatalysis. In this context, coordination polymers (CPs) and metal-

organic frameworks (MOFs) have taken more attention as candidates as photocatalytic materials by the virtue of their unique properties of large surface area and/or small band gap [5].

Many researchers have developed CPs and MOFs for photocatalytic degradation of organic dyes. To name a few, Liming Fan *et al.* synthesized five different coordination polymers based on rigid tetra carboxylic acids and imidazole linkers using Cu, Ni, Co, and Zn as nodes. The produced CPs achieved degradation efficiency of up to 97.3%for MB after 2 hours[6]. Lei-Lei *et al.* constructed five different Zn(II)/Cd(II) coordination polymers derived from a new linear carboxylate/pyridyl ligand; (pyridin-3-yl)methyl 4-(2-(4-((pyridin-3-yl) methoxy) phenyl) diazenyl) benzoate. The photocatalytic activities of the produced CPs were evaluated by degradation of MB (initial concentration: 12.5 ppm) under UV-Vis light irradiation and the results showed that a degradation efficiency of 95% with MB in 120 min could be reached [7].

Imidazole and substituted imidazoles have been considered as building blocks and linkers for the construction of many coordination networks. Typically, they are widely used to synthesize MOFs with zeolite-like structures. These MOFs are called ZIFs and are intended for specific functions[8, 9].The N-imine atom of the imidazole ring bears lone pair of electrons and can serve as an electron donor for Lewis acidic metal ions, whereas the N-pyrrole atom can be converted to Lewis base by deprotonation under basic conditions forming imidazolate anion that has the ability to act as a bidentate bridging ligand [10]. In this context, ammonia solution (33%wt., pK_a= 37) which is more basic than imidazole (pK_a= 14.5) has been used in the synthesis process for the deprotonation of imidazole before coordination.
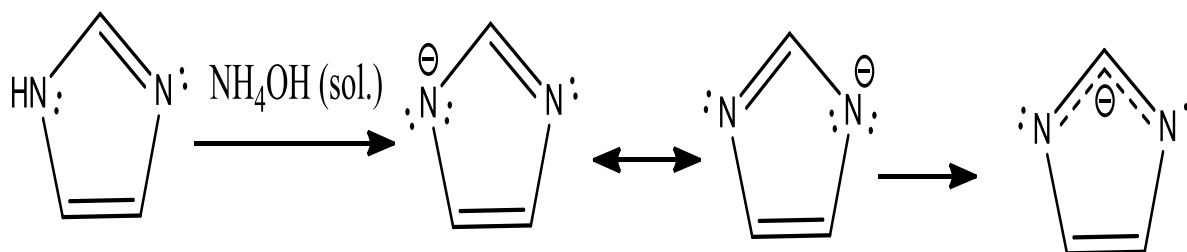
In this work, we synthesized Zn-Im CP and then evaluated its photodegradation activity towards organic dyes under visible light irradiation. MB, which is difficult to be degraded naturally, was utilized as model dye contaminant, and the kinetics of the catalytic photodegradation reactions was investigated as well.

2. Experimental

2.1. Synthesis of Zn-Im
Imidazole (extra pure, Oxford), zinc acetate dehydrate (extra pure, Sigma), ammonia solution (33%wt., Piochem), and distilled water were used in this work. Imidazole (2 mmol, 136 mg/10 ml distilled water)and ammonia solution (3 drops, 33%wt.) were added in a 100 ml Pyrex glass reactor. The mixture was left for 10 minutes and then zinc acetate (1 mmol, 219 mg/10 ml distilled water) was added resulting in a slight turbidity. The reactor was tightly closed and placed into a pre-heated oven at 70°C. After about two hours, the product (Zn-Im CP) started to precipitate as white hollow cubic crystals. The sample was collected and washed four times with distilled water. Finally, the Zn-Im CP sample were dried at 80°C, and then stored for later use; characterizations and photocatalytic degradation experiments.

2.2. Characterization of Zn-Im

The synthesized Zn-Im CP was characterized using several techniques: (i) crystalline nature was examined by powder X-ray diffraction (PXRD, Shimadzu XD-l) and structure determination was accomplished by phase match search of the experimental PXRD spectrum using QualX software against Cambridge Crystallography Open Database (COD), (ii) chemical structure was investigated by FTIR (using standard KBr pellet method, recording range 500 to 3500 cm^{-1}, Jasco FT/IR 4100. The surface morphology of Zn-Im CP was visualized using SEM (Zeiss EVO-10microscopy) and the coupled (EDX) was applied to analyze the chemical composition. Surface area of Zn-Im CP was determined by BET analysis (NOVA Station A). UV-VIS/DRs spectra were recorded using (Jasco V 530 spectrometer, Japan).

2.3. Assessment of photocatalytic versus photolytic decomposition
To obtain relevant information about the photocatalytic degradation, it was important to carry out some preliminary photolysis experiments to examine its efficiency without catalyst. The decomposition of MB by visible light was studied in two cases. The first case was the decomposition in the absence of catalyst which is called the photolysis process and the second case was the decomposition in the presence of catalyst which is called the photocatalytic process. The photolytic decomposition of MB (25 ml of aqueous solution, concentration 5 ppm) was conducted in a 100 ml beaker top-exposed to the led lamp radiation (light spectrum in the range 400-800 nm, 35 W). To perform the photocatalytic decomposition experiments, the same amount and concentration of MB with specific amount of Zn-Im CP (50 mg) were loaded into the 100ml beaker and irradiated by the led lamp radiation. In both experiments, aliquots of 3 ml were sampled using a micropipette at specified time intervals. The aliquots samples were analyzed immediately using carry Agilent 60 UV–Vis spectrophotometer.

The photodecomposition efficiency of the contaminant (η) was calculated from the following equation:

$$\eta = \left(\frac{C_{\mathrm{o}} - C_{\mathrm{t}}}{C_{\mathrm{o}}} \right) \times 100$$

Where C_o is the initial concentration of the contaminant (mg/l), and C_t is the concentration at time (t).

The effect of pH on the photodegradation process was studied as solution pH markedly influences the overall efficiency of the photocatalytic processes. To study the influence of solution pH on the initial photocatalytic decomposition rate of contaminants, the photocatalytic decomposition experiments of MB were carried out at three different pH values to cover the whole pH range of aqueous solutions; 4 (acidic), 7.5 (nearly neutral) and 10 (basic).

3. Result and discussion

3.1. Characterization of Zn-Im CP
Figure.1 shows the SEM image of Zn-Im CP where particles have a shape of being regular-ribbed interestingly with longitudinal holes.

The particles edges are about 20μm. According to EDX spectrum, figure 2. the synthesized Zn-Im CP is composed of the elements (% atom) of Zn (5.5), C (55), N (35) and O (4.18) and no other elements were detected. The elemental ratios can be given as: Zn(1): C(10): N(7): O(0.76) Accordingly, carbon to nitrogen ratio in Zn-Im CP (about 1.5:1) is similar to that of imidazole molecule which suggests the intact presence of imidazole in Zn-Im CP structure.
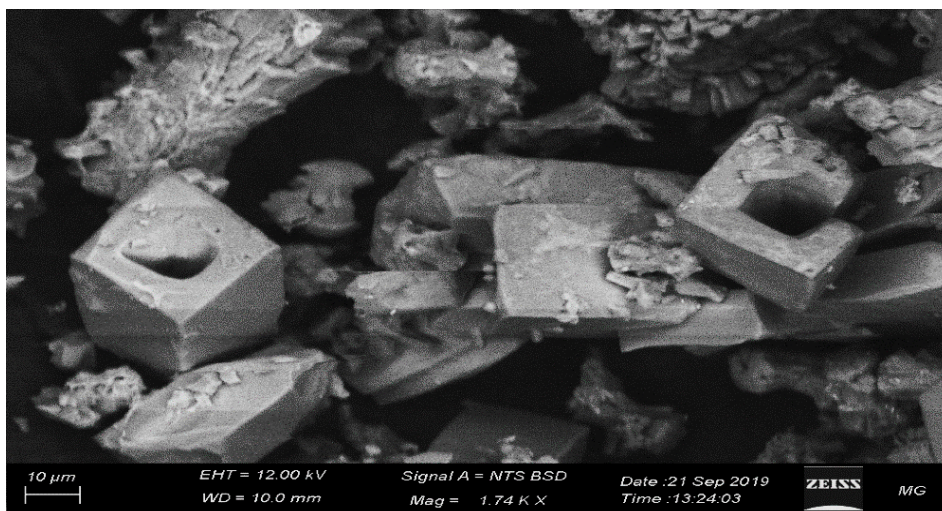
Figure 1. SEM image of the as-synthesized Zn-Im CP
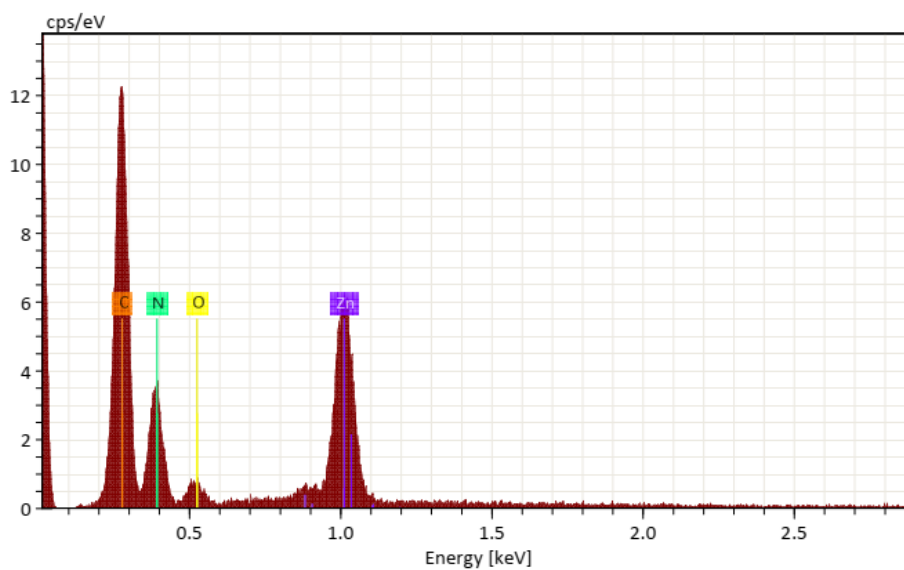

Figure 2. EDX spectrum of Zn-Im CP

The FTIR spectra of imidazole and Zn-Im CP are shown in figure.3. The spectrum of imidazole illustrates its known characteristic peaks: C–H stretching vibrations in the regions 3090-3140 cm^{-1} and 2900-2950 cm^{-1}.The two peaks appearing at 3095 and 2900 cm^{-1} obviously disappeared in the new Zn-Im CP spectrum giving an indication of developing new structure of imidazole with increased rigidity due to coordination with the metal nodes[11, 12].

The N−H stretching vibration over the broad region from 2500-3000 cm^{-1} with two characteristic peaks at 2901 and 2995cm^{-1} [13-15].When imidazole reacts completely with metallic ions, these peaks have been reported to disappear from the CPs spectra confirming the modification of imidazole structure due to deprotonation process and formation of coordination bonds with zinc.

The peaks at 1457and 1365cm^{-1} in imidazole should be designated to C−N stretching mode of vibration [12, 14].These peaks have been shifted to 1491 and 1367cm^{-1}in the Zn-Im CP spectrum which means that imidazole moiety is still found in the new product. The stretching modes of C=N and C=C are observed in the broad region from1500 to 1600 cm^{-1} with two characteristic peaks at 1540 and 1569 cm^{-1}. These two peaks are observed at 1585 and 1610 cm^{-1} in the case of CP. Such observed shift is relevant to higher energy band implying an increase of imidazole ring rigidity due to the formation of new coordination chains that affect the ring coherence [11, 14, 15].

The C−H out-of-plane-bending strong peaks appearing at 1048 and 1095 cm^{-1} in imidazole are shifted to 1086 cm^{-1} in the Zn-Im CP which manifest the existence of intact imidazole in the structure[15, 16].The presence of the broad band at the region from 3200 to 3550 cm^{-1} is an indication for the existence of OH group [13, 17].
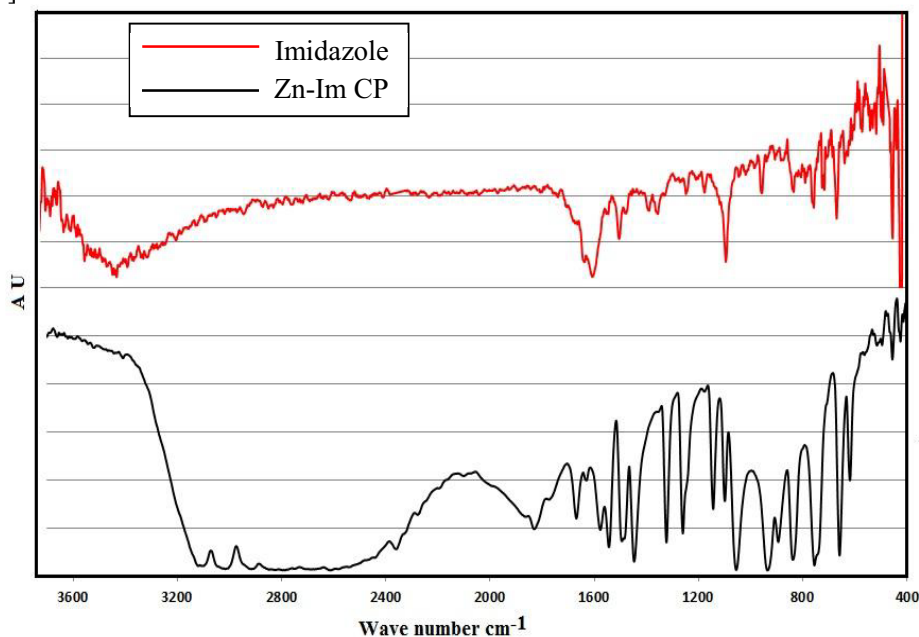

Figure 3. FT-IR spectra of the synthesized Zn-Im CP and imidazole

BET analysis, using N_2 as molecular probe of Zn-Im CP gives a surface area of about 1.1 m^2/g which is considerably low. This value indicates the non-porous nature of Zn-Im CP structure. However the photocatalytic degradation of dyes gave good results, as will be shown later, which suggests that the photocatalytic degradation mechanism does not basically depend on adsorption step. UV-Vis diffuse reflectance of Zn-Im CP is shown in figure 4.
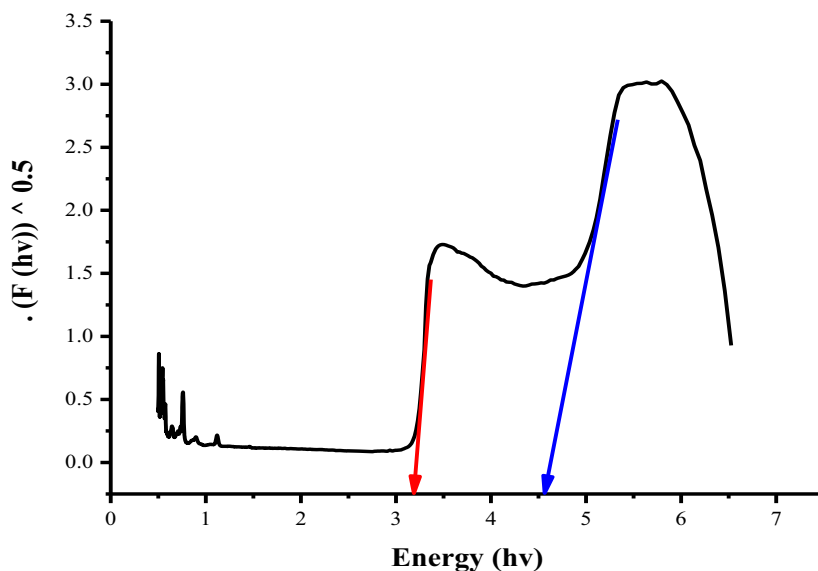
Figure 4. Diffuse reflectance for Zn-Im CP

The band gap value (E_g) was calculated from the plot of $(F(h\nu))^{0.5}$ versus $h\nu$ where $F=(1-R)/(2R)$, R is reflectance , h is Plank's constant, and ν is the frequency [18, 19]. The calculated E_g values are 3.15 and 4.6 eV. The smaller band gap, 3.15 eV, nominates the Zn-Im CP to be active under the irradiation with visible light.

Figure 5 shows XRD pattern of Zn-Im CP. It is clear that the synthesized Zn-Im CP is highly crystalline due to the sharp peaks of its spectrum. This high crystallinity provides the privilege of high charge mobility upon excitation. In addition, it shows the suitable choice of ammonia as deprotonating agent in the synthesis.

To determine the structure of the synthesized Zn-Im CP, its powder XRD pattern was exported to the phase identification software (QualX, version 2.24) which uses the crystallography open database (COD) for search match. The search match resulted in zinc imidazolate structure, chemical formula ($C_{12}H_{12}N_8Zn_2$), with figure of merit value of 0.82. The cif file of the compound was imported from Cambridge Crystallography Data Centre (CCDD) and further refined against the experimental PXRD spectrum via Materials Studio software (Biova, USA) to extract the experimental parameters using Pawley refinement. table 1 gives the structure parameters of Zn-Im CP where its cell is tetragonal with volume of 6788.81A^3 and it crystallizes in I 41 C D space group. The formula unit of the compound is $[Zn(Im)_2]_n$ and there are 16 formula unit in the cell. table 2 lists the experimental parameters of PXRD measurement.

Figure.6 compares the experimental PXRD pattern of the proposed CP to the experimental one. It is obvious that the two patterns highly coincide and the difference between them is very small. This is reflected in the lower value of R_wp (10.30%), which is a measure of the degree of matching between the simulated pattern and experimental one. Figure. 7 visualizes the chemical structure of the synthesized Zn-Im CP where Zn atoms (in red) are tetrahedrally coordinated to four imidazole rings.
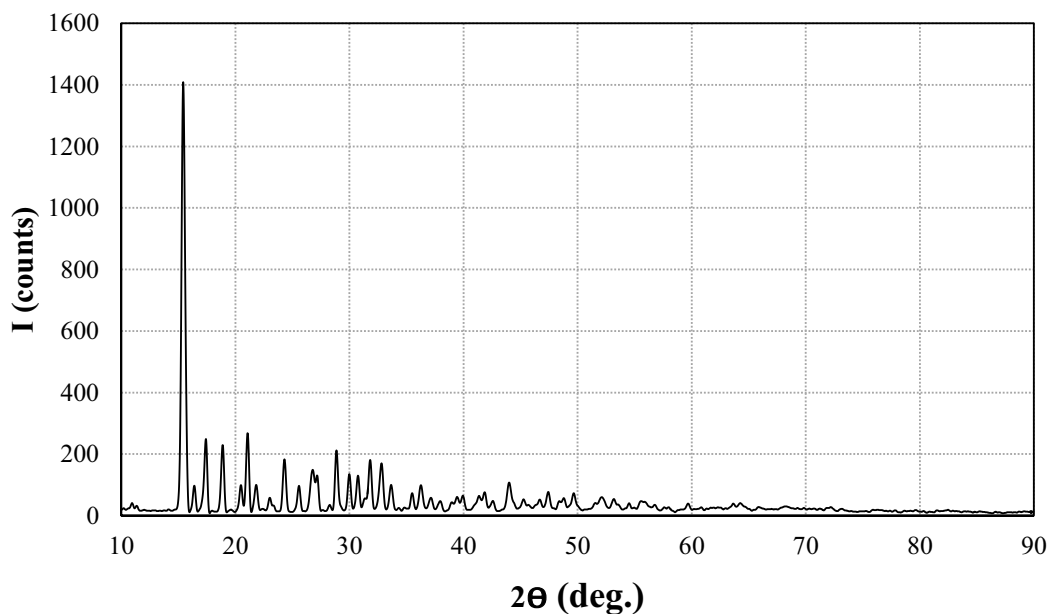
Figure 5. XRD powder patterns of Zn-Im CP

Table 1: structural parameters of Zn-Im CP

Parameter	Value	Parameter	Value
Lattice Type	Tetragonal	Space Group	I 41 C D
a	23.36	Cell Volume (A^3)	6788.81
b	23.36	Density (g/cm^3)	1.56
c	12.4	2θ Range (degrees)	5.02-89.98
α	90.0	Step Size (degrees)	0.04
β	90.0	Number of Reflections	734
γ	90.0	Final R_p	7.09%
Z	16	Final R_{wp}	10.30%

Table 2: PXRD experimental parameters

FWHM	
U	1.06144 ± 0.04530
V	-0.43825 ± 0.02825
W	0.14136 ± 0.00421
Profile Function: Pseudo-Voigt	
NA	0.00000 ± 0.01133
NB	-0.00000 ± 0.00040
Line Shift Instrument Geometry: Bragg-Brentano	
Zero Point	0.17007 ± 0.00172
Asymmetry Correction: Berar-Baldinozzi 2θ Limit: 30 (degrees)	
P1	-0.01770 ± 0.03911
P2	0.17957 ± 0.00815
P3	0.11348 ± 0.07320
P4	-0.38424 ± 0.01747
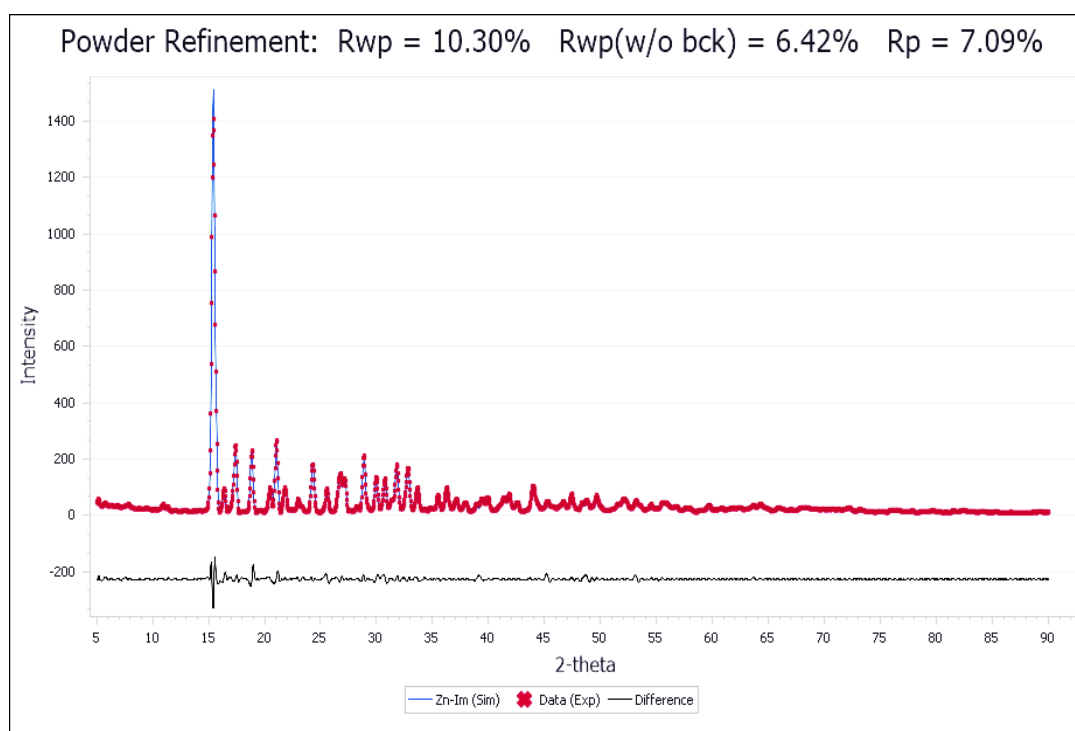
Figure 6.PXRD spectrum: a) experimental; b) simulated; and c) difference
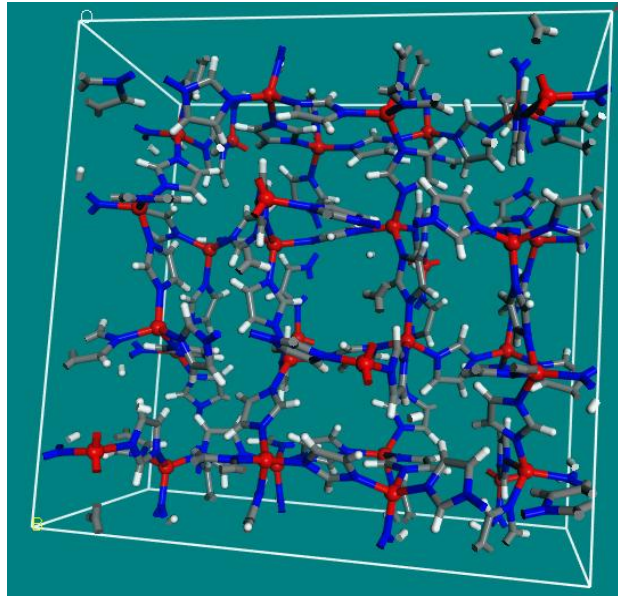
Figure 7: Chemical structure of Zn-Im CP

3.2. Photocatalytic degradation of MB by Zn-Im CP
3.2.1. Photolytic versus photocatalytic degradation of the MB.
Figure.8 shows the change in decomposition efficiency with time for MB under visible light in the absence/presence of Zn-Im CP. In absence of Zn-Im CP experiment indicated a decomposition efficiency of 66 % was recorded after 300 min. as a result of photolysis process. In presence of Zn-Im CP experiment derived decomposition through photocatalytic process which raises the efficiency to 90% within the same period of illumination.
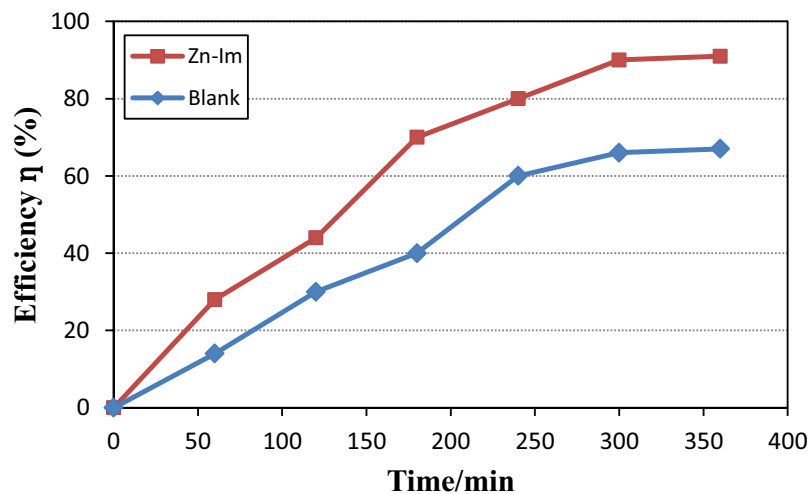

Figure 8. Photolytic and photocatalytic degradation of the MB solution (pH= 7.5).

3.2.2. Effect of pH on the photocatalytic process

The pH dependence of photocatalysis can be associated with changes of the surface charge of the photocatalyst, net charge of pollutant, changes in its adsorption modes, and amount of produced hydroxyl radicals. These changes can lead to a modification of the overall rate of decomposition [20]. Additionally, the change in pH may cause intermediates formation that could poison the photocatalyst [20, 21].
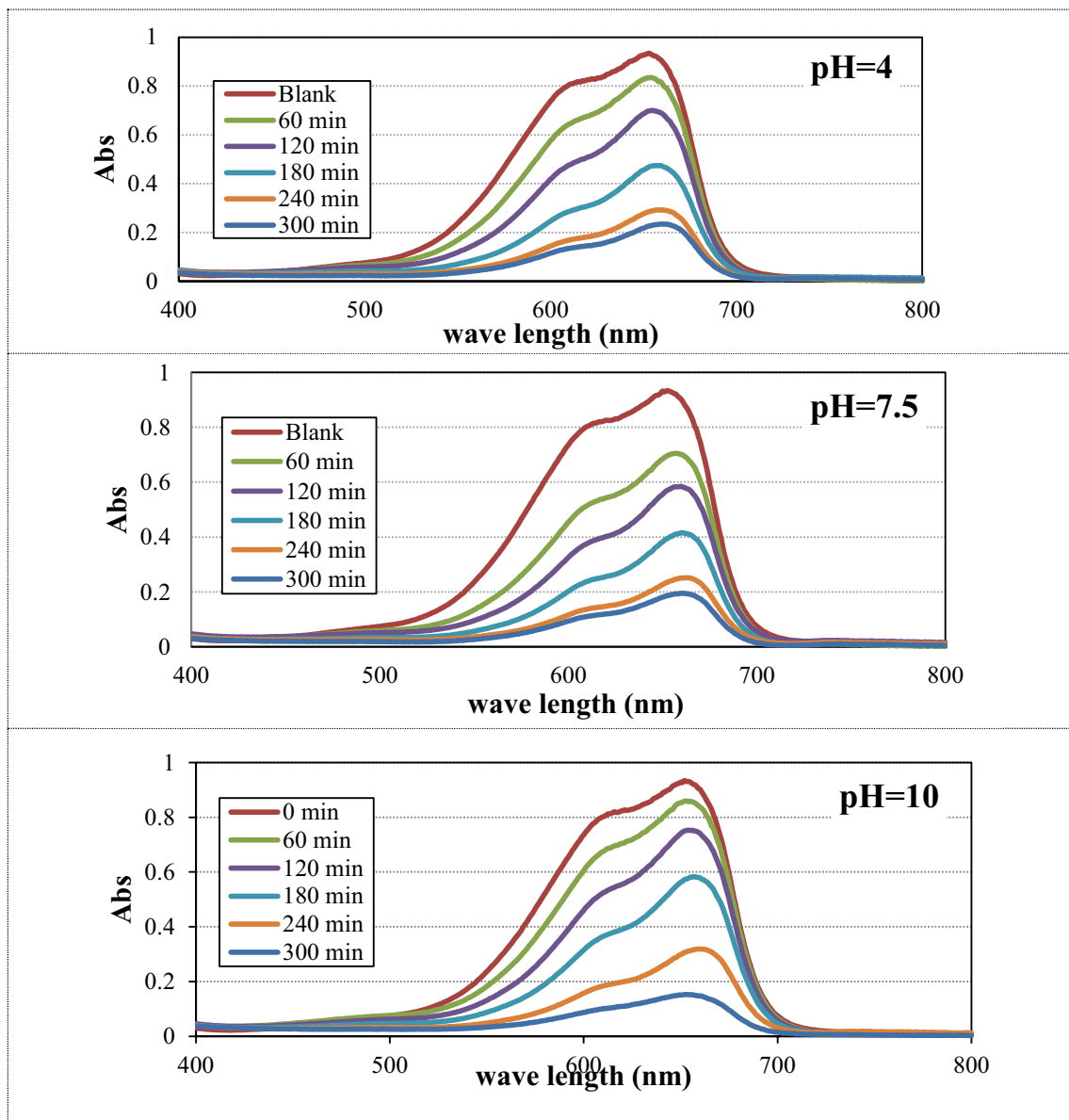

Figure 9. UV–vis absorption spectra of MB solution during photo catalytic degradation using (Zn-Im CP) catalyst under visible light at different pH.
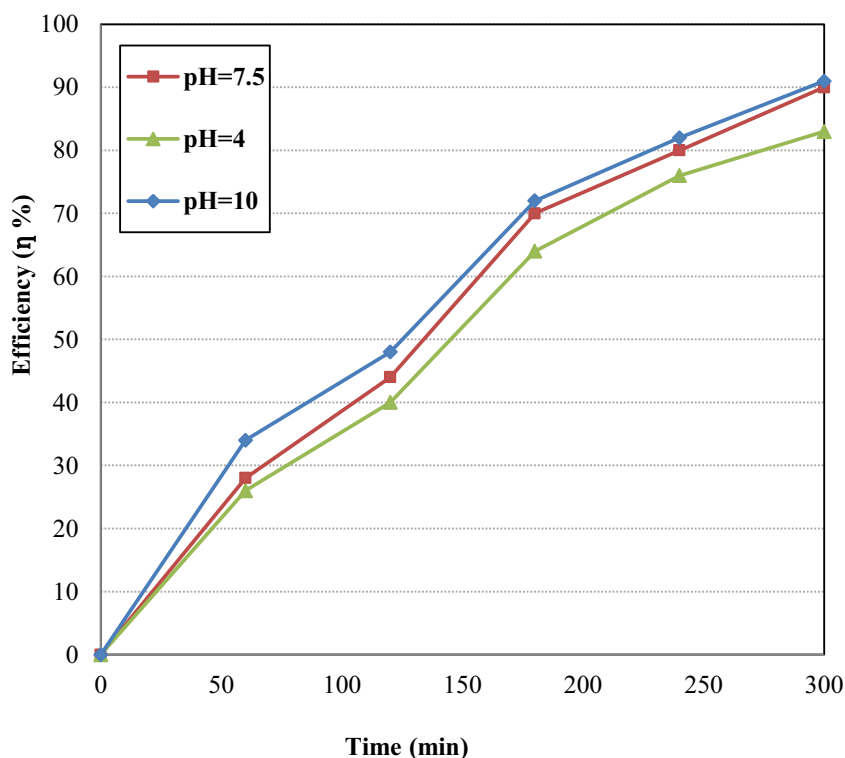
Figure 10. Photo catalytic degradation of the MB solution at different pH

To study the effect of pH on the degradation efficiency, three sets of experiments were performed fixing all experimental conditions except for the pH. For each experiment, specific amount of the solution was withdrawn at definite time intervals and the absorbance of the solution was measured using UV-VIS spectrometer over the range 400-800 nm. The results of these experiments are shown in figure 9.The results illustrate that Zn-Im CP photo-degraded MB effectively under visible light irradiation as indicated by the significant reduction in MB peak at 664 nm after irradiation period of 300 minute.

For each pH value, the maximum absorbance, occurring at 664 nm, was extracted for all curves and converted into concentration unit which was finally plotted against its corresponding time. The output is displayed in figure 10 which shows the change in MB concentration with time during visible light irradiation in the presence of Zn-Im CP at different pH values. It is observed that the degradation rate at all pH is very close to each other which indicate the non-effectiveness of changing medium pH on our CP.

3.2.3. Assessment of degradation with respect to initial pH

The pH of the solution plays an important role in the degradation rate of dyes. At high pH (basic medium), the degradation rate at first 120 min was higher than others, that's might be due to the presence of plenty of hydroxyl groups ($^-$OH) which is the main source of ($^\cdot$OH) that is responsible for dyes degradation according to degradation mechanism scheme given below [4, 22].In contrast, in acidic medium, the presence of plenty of H$^+$ will cause repulsion forces with the cationic dye (MB$^+$) limiting its approach to the Zn-Im CP surface, hence yielding low degradation rate.

3.2.4. Photocatalytic degradation mechanism for MB

A simplified model of photocatalytic degradation based on indirect mechanism pathway is presented in Figure. 11. When the Zn-Im CP was irradiated with the visible light, the electrons (e^-) in the valence band (VB) were excited to the conduction band (CB), at the same time the same number of holes that have been produced (h^+) were left in VB. At VB the plenty of h^+ interact with water molecules providing ultimately $^\cdot$OH which oxidizes of MB. Simultaneously, at CB, the excited electrons inject into adsorbed oxygen molecules on the surface of the Zn-Im CP to form $^\cdot O_2^-$ which converts to $^\cdot$OH causing MB oxidation.

In order to investigate the kinetics of the photocatalytic degradation in neutral medium, the pseudo first order model was applied, $\ln(C_o/C)=kt$, where C_o and C are the initial and the remaining concentrations of MB at regular time intervals respectively and k is the rate constant. Plots of ln (C_o/C) against t were drawn for pH 7.5. From the plots, k was determined at pH=7.5 According to fitted equation, $k= 0.006$ min^{-1}. Table 3, gives the rate constants of photocatalytic degradation of MB (initial pH=7.5) by Zn-Im CP compared to some other photocatalysts, indicates a moderate performance of Zn-Im CP.
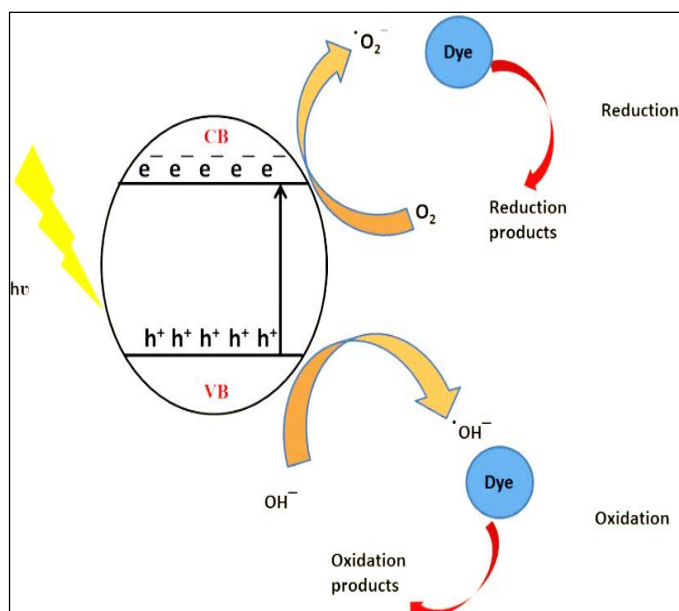

Figure 11.Simplified photocatalytic reaction mechanism of the MB solution on CPs.

Table 3: Rate constants of photocatalytic degradation of MB (initial pH=7.5)

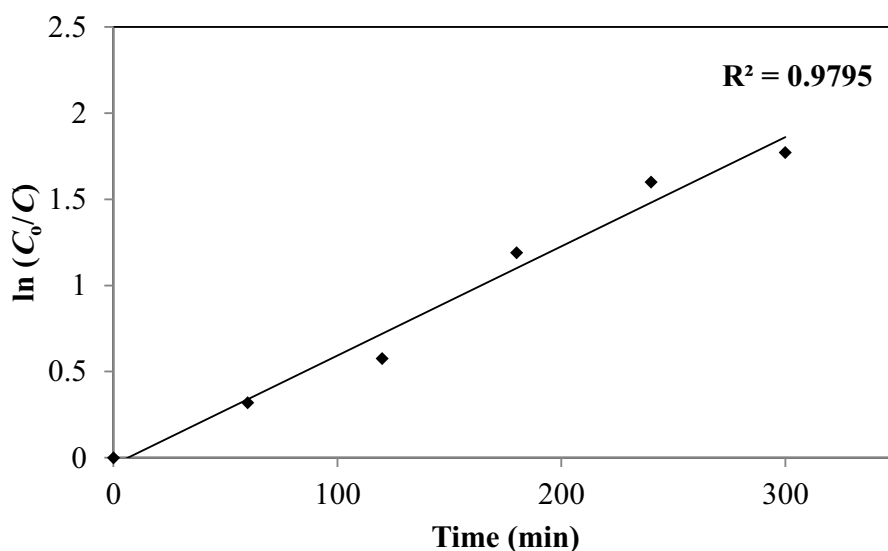| Dye	k (min^{-1})*			
	This work	[18]	[23]	[24]
MB	0.006 (R^2=0.979)	0.0110	0.00435	0.00194

Figure 12.First-order kinetic plot for the photocatalytic degradation of MB using Zn-Im CP as catalyst under visible light irradiation.

4. Conclusion

The coordination polymer Zn-Im CP based on zinc acetate and imidazole was simply synthesized using ammonia as deprotonating agent at comparatively low temperature, 70°C. Zn-Im CP is highly crystalline which provides the privilege of high charge mobility upon excitation, hence suitable photocatalysis. Zn-Im CP shows two band gap values where $E_g = 3.15$ eV should be responsible for excitation under visible irradiation. For the three initial pH, 4, 7.5, and 10, Zn-Im CP show stable photodegradation of MB from 83%-91%. The rate constant is 0.006 min^{-1} which is comparable to the rates of many other photocatalysts.

References

[1]   Yang, Y. and J. Luan, *Synthesis, property characterization and photocatalytic activity of the novel composite polymer polyaniline/Bi2SnTiO7.* Molecules, 2012. **17**(3): p. 2752-2772.
[2]   Rauf, M. and S.S. Ashraf, *Fundamental principles and application of heterogeneous photocatalytic degradation of dyes in solution.* Chemical engineering journal, 2009. **151**(1-3): p. 10-18.
[3]   Muhammad, A.S., et al., *Effects of Operating Parameters on Photocatalytic Degradation of Methylene Blue or Phenol on Supported Titanium-Based Catalysts.* Asian Journal of Chemistry, 2015. **27**(1): p. 313-320.
[4]   Sakthivel, S., et al., *Solar photocatalytic degradation of azo dye: comparison of photocatalytic efficiency of ZnO and TiO2.* Solar energy materials and solar cells, 2003. **77**(1): p. 65-82.
[5]   Wen, L.-L., et al., *Structures, photoluminescence, and photocatalytic properties of six new metal−organic frameworks based on aromatic polycarboxylate acids and rigid imidazole-based synthons.* Crystal Growth and Design, 2009. **9**(8): p. 3581-3589.

[6]   Fan, L., et al., *Coligand syntheses, crystal structures, luminescence and photocatalytic properties of five coordination polymers based on rigid tetracarboxylic acids and imidazole linkers.* CrystEngComm, 2015. **17**(48): p. 9413-9422.

[7]   Liu, L.-L., et al., *Construction of five Zn (II)/Cd (II) coordination polymers derived from a new linear carboxylate/pyridyl ligand: design, synthesis, and photocatalytic properties.* Dalton Transactions, 2016. **45**(31): p. 12352-12361.

[8]   He, Y., et al., *Multifunctional metal–organic frameworks constructed from meta-benzenedicarboxylate units.* Chemical Society Reviews, 2014. **43**(16): p. 5618-5656.

[9]   Eddaoudi, M., et al., *Zeolite-like metal–organic frameworks (ZMOFs): design, synthesis, and properties.* Chemical Society Reviews, 2015. **44**(1): p. 228-249.

[10] Chen, S.-S., *The roles of imidazole ligands in coordination supramolecular systems.* CrystEngComm, 2016. **18**(35): p. 6543-6565.

[11] Hu, Y., et al., *In situ high pressure study of ZIF-8 by FTIR spectroscopy.* Chemical Communications, 2011. **47**(47): p. 12694-12696.

[12] Ramasamy, R., *Vibrational spectroscopic studies of imidazole.* Armenian Journal of Physics, 2015. **8**(1): p. 51-55.

[13] Omrani, A., et al., *Study on curing mechanism of DGEBA/nickel–imidazole system.* Thermochimica Acta, 2008. **468**(1-2): p. 39-48.

[14] Drolet, D.P., et al., *FT-IR and XPS study of copper (II) complexes of imidazole and benzimidazole.* Inorganica Chimica Acta, 1988. **146**(2): p. 173-180.

[15] Morzyk-Ociepa, B., E. Różycka-Sokołowska, and D. Michalska, *Revised crystal and molecular structure, FT-IR spectra and DFT studies of chlorotetrakis (imidazole) copper (II) chloride.* Journal of Molecular Structure, 2012. **1028**: p. 49-56.

[16] Fernández-Bertrán, J., et al., *Proton transfer in solid state: mechanochemical reactions of imidazole with metallic oxides.* Journal of Solid State Chemistry, 1999. **147**(2): p. 561-564.

[17] Suh, M.P., B.Y. Shim, and T.-S. Yoon, *Template syntheses and crystal structures of nickel (II) complexes of hexaaza macrocyclic ligands with pendant functional groups: formation of a coordination polymer.* Inorganic Chemistry, 1994. **33**(24): p. 5509-5514.

[18] Yang, Y.-J., et al., *Synthesis and characterization of two 3D supramolecular cadmium (II) coordination polymers based on aromatic polycarboxylate and semi-rigidity bis (imidazole) ligands.* Polyhedron, 2018. **156**: p. 72-79.

[19] Nada, A.A., et al., *Elaboration of nano titania-magnetic reduced graphene oxide for degradation of tartrazine dye in aqueous solution.* Solid State Sciences, 2018. **78**: p. 116-125.

[20] Carp, O., C.L. Huisman, and A. Reller, *Photoinduced reactivity of titanium dioxide.* Progress in solid state chemistry, 2004. **32**(1-2): p. 33-177.

[21] Evgenidou, E., K. Fytianos, and I. Poulios, *Photocatalytic oxidation of dimethoate in aqueous solutions.* Journal of Photochemistry and Photobiology A: Chemistry, 2005. **175**(1): p. 29-38.

[22] Doong, R.-A., et al., *The influence of pH and cadmium sulfide on the photocatalytic degradation of 2-chlorophenol in titanium dioxide suspensions.* Water research, 2001. **35**(12): p. 2873-2880.

[23] Luan, J. and Y. Zhuang, *Synthesis, Structural Property, Photophysical Property, Photocatalytic Property of Novel ZnBiErO4 under Visible Light Irradiation.* Materials, 2018. **11**(2): p. 303.

[24] Pu, Y., et al., *Visible-Light-Induced Degradation of Methylene Blue by SrBi3VO8 Nanoparticles.* Journal of the American Ceramic Society, 2015. **98**(8): p. 2528-2533.